

Provenance Evolution and Its Response to Sea Level Change in the South Yellow Sea since 1.0 Ma

Zhonglei Wang^{a, b, *} (ORCID: 0000-0002-0802-0976), Yong Zhang^{a, **, 1}, Beibei Mi^a, Zhongbo Wang^c,
Yanguang Dou^{a, b}, Jingyi Cong^a, and Jun Sun^a

^a Qingdao Institute of Marine Geology, China Geological Survey, Qingdao, China

^b Laoshan Laboratory, Qingdao, China

^c Institute of Marine Sciences, Guangdong Provincial Key Laboratory of the Marine Disaster Prediction and Prevention, Shantou University, Shantou, China

*e-mail: wzhl2010@sina.cn

**e-mail: qimg829@126.com

Received December 15, 2022; revised June 2, 2023; accepted October 19, 2023

Abstract—The sediments provenance of the South Yellow Sea is controlled by many factors such as sea level change, ocean circulation, and neotectonic movement. The short time scale sediments provenance changes in this region since the Holocene have been revealed well, and a unified understanding has been formed that the central muddy area in the South Yellow Sea is a mixed area of the Yellow River sediments and the Yangtze River sediments. However, the contribution of different rivers to the sediments of the South Yellow Sea since late Quaternary is still ambiguous. Through comparative analysis of several boreholes with precise annual data constraints in the central mud area, the process of sediments provenance change at different periods since the late Early Pleistocene (1.0 Ma) was reconstructed, and the coupling mechanism of sediments provenance change and sea level change was established. It is found that during the period from 1.0 to 0.88 Ma, the seawater entered the South Yellow Sea along the Yellow Sea trough from the southeast to north as a channel, and there were different phenomena at the same time in different regions. Since 0.88 Ma, the sea water has been advancing from east to west. In addition, the sediments in the western of Jeju Island are mainly from China, and the sediments in the eastern are mainly from the Korean Peninsula, which roughly coincides with the boundary between the silty area and the sandy area on the eastern of the South Yellow Sea. In the surface sediments, the boundary line between the Yellow River sediments and the Yangtze River sediments is approximately 33.4° N.

Keywords: South Yellow Sea, late Early Pleistocene, provenance, detrital zircon, sea level change

DOI: 10.1134/S1819714024010081

1. INTRODUCTION

The process of river sediments source to sink in the East Asian continental margin is a major scientific issue in the field of Earth sciences [1]. The evolution of this large-scale source to sink system has been recorded in the sedimentary stratigraphy of the shallow continental shelf in east China seas, which has been an important information carrier for the reconstruction of the tectonic uplift, monsoon evolution and climate change of the Asian continent in the Cenozoic [2–4]. Meanwhile, shallow-sea shelf sedimentary records are also important indicators of global sea level change [5–7].

The Yellow Sea is a typical semi-enclosed continental shelf sea, and its surrounding rivers mainly include the Yangtze River, Huaihe River and Yellow River in China and Han River and Geum River in

Korean Peninsula, receiving a large number of terrigenous detrital materials from the rivers [8]. Under the control of sea currents such as Yellow Sea Warm Current and Yellow Sea Coastal Current and cold water masses, several muddy areas were formed in the western of the North Yellow Sea, the central of the South Yellow Sea, the southwest of Jeju Island and the southeast of the South Yellow Sea [9]. Among them, the muddy area in the central of the South Yellow Sea has the most study results. Based on mineralogical and geochemical evidence, most scholars believe that the sediments in the muddy area in the central of the South Yellow Sea are mainly supplied by the Yellow River and the Yangtze River [8, 10–14]. Other potential sources are local small rivers, such as the Huaihe River, whose annual sediment fluxes to the sea is relatively low (~76 Mt/yr) and may contribute little to the central mud area [15]. Rivers originating from the Korean Peninsula, such as the Han River and the

¹ Corresponding author.

Geum River, transported sediment flux to the eastern Yellow Sea of only 18 Mt/yr [15], and contributed little to the central mud area sediments [8]. In addition, the influence of aeolian dust on the deposition of the South Yellow Sea is negligible due to the dilution of the huge amount of sediment from the Yellow River and Yangtze River [16]. Based on the study of NHH01 borehole, it was found that the sediments provenance in the South Yellow Sea was mainly controlled by the Yellow River since 0.88 Ma [17]. Detrital zircon U-Pb age analysis from CSDP-1 borehole showed that the Yellow River sediments only began to appear in the central mud area at 0.78 Ma, and since then the Yellow River has become the main provenance in the drilled area [18]. Zhang et al. proposed by studying the clay minerals of the CSDP-1 borehole that the large-scale transgressions of the Yellow Sea and Bohai Sea occurred roughly synchronously in the Quaternary [19], at about 0.8 Ma. The provenance of the South Yellow Sea sediments from 3.5 to 0.8 Ma is mainly from the old Yangtze River, but since 0.8 Ma ago it is mainly from the Yellow River. It is speculated that the Yellow River has affected the South Yellow Sea since the Middle Pleistocene at least.

The sediments provenance in the South Yellow Sea is controlled by many factors such as sea level change and neotectonic movement, which is one of the most important scientific problems in this area. Most results of the early research were based on fine sediment ($<2\ \mu\text{m}$). The short time scale provenance changes in this region since the Holocene have been revealed well, and a uni-

fied understanding has been formed that the central muddy area in the South Yellow Sea is a mixed area of the Yellow River sediments and the Yangtze River sediments. However, the contribution of different rivers to the sediments of the South Yellow Sea since late Quaternary is still ambiguous.

2. GEOLOGICAL SETTING

The South Yellow Sea lies between China mainland and the Korean Peninsula. In terms of regional structure, the South Yellow Sea shelf is located in the Lower Yangtze plate (Fig. 1), bounded by the Qianliyan uplift in the north, the Wunansha uplift in the south, the Tanlu fault zone in the west, and the Korean Peninsula in the east, with the Subei Basin in the land and the South Yellow Sea Basin in the sea [20–23].

The Zhe-Min Uplift is a tectonic belt spreading NEE, separating the South Yellow Sea basin and the East China Sea shelf basin. Its main body is in the east of Zhejiang Province and Fujian Province, extending northeast into the Yellow Sea and the East China Sea seabed, and connecting with the Lingnan block in the south of the Korean Peninsula through Suyan Reef and Jeju Island, with a length of 2100 km and a width of 200–300 km [24–26]. Until Jurassic, this tectonic zone has been uplifted, only volcanic rocks without clastic sediments accumulation [27]. The Yanshan Movement in the Cretaceous resulted in a series of NNE faults and faulted basins in Zhe-Min Uplift, in

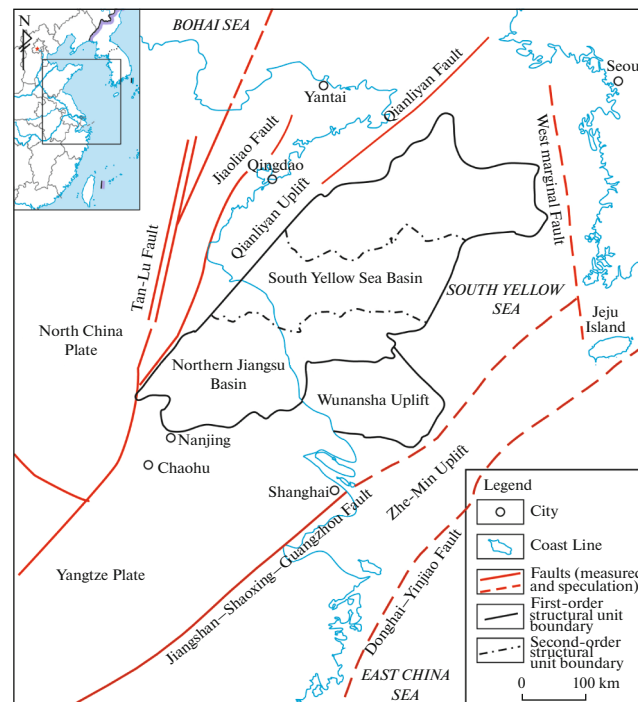


Fig. 1. Structural outline map of South Yellow Sea (According to references [29–31]).

which red sandstone, glutenite, tuffaceous glutenite and intermediate acidic volcanic rocks were accumulated. Since the Neogene, the Zhe-Min Uplift has suffered division and subsidence, and the sea water from the East China Sea crossed the Zhe-Min uplift into the Yellow Sea at about 1.66 Ma [28].

The average depth of the South Yellow Sea is 46 m, and the deepest is located in the north of Jeju Island, reaching 140 m [32]. The sea floor of the South Yellow Sea consists of six topographic units: the southern bank slope and Haizhou Bay terrace plain, the outer tongue platform of the North bank of Jiangsu, the central plain, the Yellow Sea Trough depression, the offshore platform of the Korean Peninsula and the sand ridge of the west of Jeju Island. Among them, the Yellow Sea Trough depression is located in the middle of the South Yellow Sea, close to the Korean Peninsula, which is shallow in the north and deep in the south, steep in the east and slow in the west [32], and its deepest point can reach more than 100 m. Previous studies believed that the Yellow Sea trough was formed by the flow of the last glacial age and was the main channel for seawater intrusion in the Holocene [33]. The modern Marine current system in the South Yellow Sea mainly includes Yellow Sea warm current and coastal current. The Yellow Sea cold water mass in the middle of the South Yellow Sea is a low-energy environment, which mainly distributes muddy sediments.

In the eastern and southwestern parts of the South Yellow Sea, strong tidal currents developed and formed tidal sand ridges [10].

3. MATERIALS AND METHODS

This study comprehensively analyzed studies on sediment provenance in the South Yellow Sea since late Quaternary [34–39], combined with zircon U-Pb dating of multiple borehole sediments and surface sediment samples (Fig. 2 and Table 1), summarized the sediment provenance changes since 1.0 Ma.

Zircon has strong weathering resistance and is widely distributed in terrigenous detrital sediments of various sedimentary environments in rivers, lakes and deltas. By comparing the age spectrums of multiple samples and analyzing the tectonic history and sedimentary environment characteristics of the regional basin, the transport path of sediments can be well tracked [43–47]. In the past 20 years, with the development of in situ analysis of single-particle minerals, the detrital zircon U-Pb dating method has become one of the standard methods for sediment provenance research [48–50]. In this paper, detrital zircon U-Pb ages of 11 surface samples from the southern and outer edges of the central muddy area and 5 samples from SYS90-1 borehole with a bottom age of 1.0 Ma are

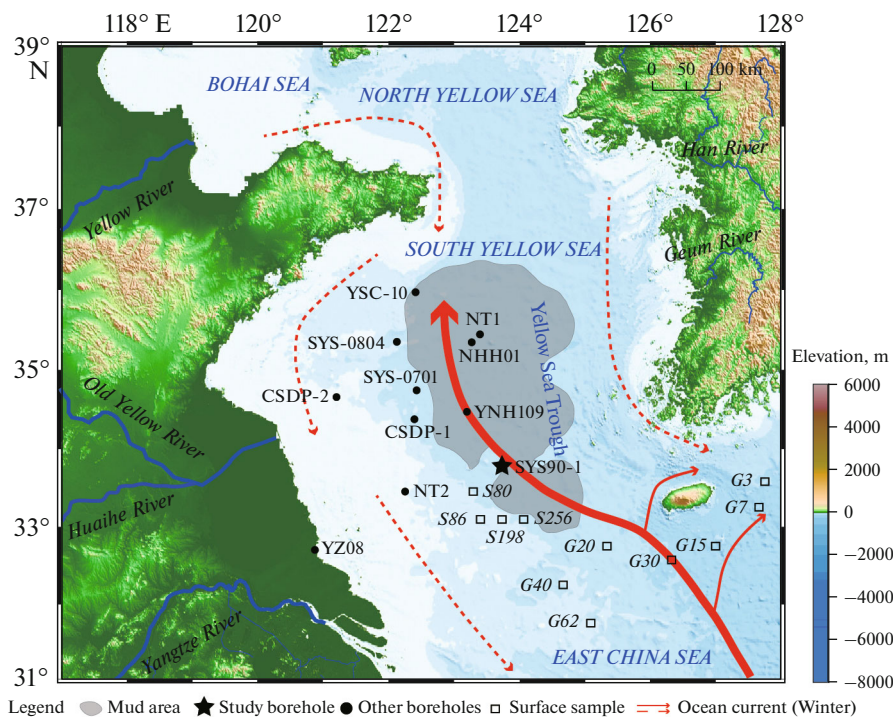


Fig. 2. South Yellow Sea and research borehole location diagram. Borehole CSDP-1 according to reference [18], borehole CSDP-2 according to reference [10], borehole NHH01 according to reference [17], borehole YNH109 according to reference [34], circulation according to reference [40], and mud area according to reference [41]. SYB80, SYB86, SYB198 and SYB256 are the surface sample sites. Surface samples G3, G7, G15, G20, G30, G40 and G62 according to reference [38].

Table 1. The main borehole information is mentioned in this study

Borehole no.	Latitude (N)	Longitude (E)	Footage, m	Depth, m	Bottom age, Ma	Reference
CSDP-1	34.30°	122.37°	300.1	52.5	3.5	[41]
CSDP-2	34.56°	121.26°	2810	22	5*	[10]
NHH01	35.22°	123.22°	125.6	73	1	[17]
SYS-0701	34.66°	122.45°	70.2	33.0	~0.16	[42]
SYS-0804	35.27°	121.15°	65.10	38.0	~0.19	[42]
NT1	35.43°	123.22°	70	74.6	~0.09	[34]
NT2	33.47°	122.25°	70.5	35.4	0.68	[35]
YSC-10	35.97°	122.42°	4.54	56.8	0.009	[36]
YZ08	32.70°	120.88°	131	0	(MIS7)	[37]
YNH109	34.47°	123.20°	3.40	73.9	>0.03	[34]
SYS90-1	33.81°	123.73°	90.1	69.3	1.0	This study

Table 2. Samples location and lithology information

Sample no.	Location	Depth, m	Lithology	Instructions	Reference
SYB80	123°17'46" E 33°27'15" N	0.20	Silt	Surface sample	This study
SYB86	124°24'17" E 33°05'40" N	0.20	Silt	Surface sample	This study
SYB198	124°44'02" E 33°05'40" N	0.20	Silt	Surface sample	This study
SYB256	124°03'48" E 33°05'40" N	0.20	Silt	Surface sample	This study
G3	127°45'05" E 33°35'05" N	0.20	Silt	Surface sample	[38]
G7	127°39'51" E 33°15'07" N	0.20	Silt	Surface sample	[38]
G15	127°00'01" E 32°45'03" N	0.20	Silt	Surface sample	[38]
G20	125°20'06" E 32°45'03" N	0.20	Silt	Surface sample	[38]
G30	126°19'51" E 32°34'57" N	0.20	Silt	Surface sample	[38]
G40	124°39'56" E 32°14'59" N	0.20	Silt	Surface sample	[38]
G62	125°05'05" E 31°44'55" N	0.20	Silt	Surface sample	[38]
SYS90-1-B709	123°43'58" E 33°48'49" N	34.88	Silt	Borehole sample	This study
SYS90-1-C717	123°43'58" E 33°48'49" N	56.20	Fine sand	Borehole sample	This study
SYS90-1-D235	123°43'58" E 33°48'49" N	68.88	Silt	Borehole sample	This study
SYS90-1-D275	123°43'58" E 33°48'49" N	69.68	Silt	Borehole sample	This study
SYS90-1-D945	123°43'58" E 33°48'49" N	85.66	Silt	Borehole sample	This study

analyzed. The studied samples location and lithology information can be seen in Table 2 and Fig. 2.

Zircon morphology analysis based on CL diagram and elemental U/Th ratio analysis show that the zircon samples are mainly of magmatic origin, which is suitable for provenance discrimination. The number of age congruent zircons in the samples is more than 90%, and the age congruent degree of zircons in the sediments used in this study is more than 90%. Zircon ages are selected according to the following principles: For ages <1000 Ma, the calculated values of $^{206}\text{Pb}/^{238}\text{U}$ are selected; for ages >1000 Ma, the calculated values of $^{207}\text{Pb}/^{206}\text{Pb}$ are selected [51].

4. RESULTS AND DISCUSSION

4.1. Zircon U-Pb Dating of Sediments

The Yellow River and the Yangtze River around the South Yellow Sea and the Han, Geum and Seomjin rivers on the Korean Peninsula may provide the main channels for the transport of seabed sediments. In this study, these rivers are used as end-members for provenance identification. The Yangtze River is the longest river in China with a wide zonal span, flowing through Changdu Block, Songpan-Ganzi fold belt, Qinling-Dabie tectonic belt, Yangtze Block and Huaxia Block from west to east [52]. The stratigraphy which it flows through is complex, distributed from Proterozoic to Quaternary. It includes a large area of carbonate rocks, terrigenous clastic rocks and intermediate acid intrusive rocks, schist and gneiss, etc. [53]. Based on a large amount of detrital zircon U-Pb age analysis, it is found that there are six major age spectrum peaks in detrital sediments from the Yangtze River: <65, 200–300, 400–550, 700–1000, 1800–2000 and 2400–2600 Ma, among which 200–300 and 700–1000 Ma were the two major age spectrum peaks [54]. As the second longest river in China, the Yellow River is famous for its great annual sediment transport. It flows through several tectonic units, including the Songpan-Ganzi orogenic belt, Qinling orogenic belt, Qilian orogenic belt and North China Block [55]. The detrital zircon U-Pb age statistics show that the detrital sediments of the Yellow River have six major age spectrum peaks: 200–350, 350–500, 700–1000, 1000–1800, 1800–2000 and 2000–2600 Ma, among which 200–350, 350–500, 1800–2000 and 2000–2600 Ma were the four major age spectrum peaks [56, 57]. Zircon U-Pb age spectrum of the main rivers on the Korean Peninsula show significant differences between the eastern and western sides of the peninsula, ranging from Early Cenozoic to late Archaean, with Paleozoic to Neoproterozoic zircons dominating in the west and Paleoproterozoic zircons dominating in the east [38].

Firstly, the KDE chart of the study samples and the surrounding river samples was drawn using IsoplotR

software [58] (Fig. 3), and the provenance of the study samples was visually interpreted.

According to Vermeesch's research, the quantitative age similarity analysis of detrital zircons U-Pb based on multi-dimensional calibration method (MDS) can effectively capture the age distribution and has strong practicability [59]. Based on the D value of Kolmogorov-Smirnoff (K-S) test or the V value of Kuiper test, the method projects the analysis results in the form of points into a multidimensional space (two-dimensional or three-dimensional) by using a specific algorithm to represent the relative differences between multiple samples, thus significantly improving the visualization of the quantitative analysis results of detrital zircon samples. The difference (δ) matrix between samples is converted by the function f into a difference matrix represented by linear distance (d), which is defined as follows for the two samples i and j :

$$d_{ij} \approx f(\delta_{ij}). \quad (1)$$

In Formula (1), $f(\delta_{ij})$ is a monotone increasing conversion function, that is, the greater the difference between samples i and j , the greater the distance between points representing the two samples in multidimensional space. MDS uses these difference matrices to project the sample points in two-dimensional or three-dimensional space and draw a graph. In this paper, IsoplotR software was used to draw the MDS chart of the study samples and the Yangtze River, Yellow River, Han River, Geum River, Seomjin River and other rivers on the Korean Peninsula (Fig. 3).

4.2. Study on Provenance Tracing of Borehole Sediments and Surface Sediments

4.2.1. Provenance tracing of borehole sediments since 1.0 Ma. The CSDP-2 hole in the South Yellow Sea that penetrated the Quaternary showed that the first transgression occurred at about 1.66 Ma, and the South Yellow Sea was dominated by fluvial facies deposition during the period of 1.66–0.83 Ma, with three weak transgressions. It was not until 0.83 Ma that the transgression intensity of the South Yellow Sea reached the present level due to the further subsidence of the Zhe-Min uplift [10, 41]. However, the transgression range of the western shelf of the South Yellow Sea during MIS5 was wider than that of the present [10].

Detrital zircon U-Pb age statistics were used to analyze the sediment provenance of SYS90-1 borehole. According to the analysis results, SYS90-1 borehole can be divided into three parts (Fig. 4). The sediments in the first part from the bottom of the borehole to the depth of 69.68 m may come from the Yellow River. According to the results of CSDP-1, CSDP-2 and NHH01 boreholes, the appearance of Yellow River sediments in the South Yellow Sea indicates that transgression occurred. The paleomagnetic results show that the bottom age of SYS90-1 borehole is

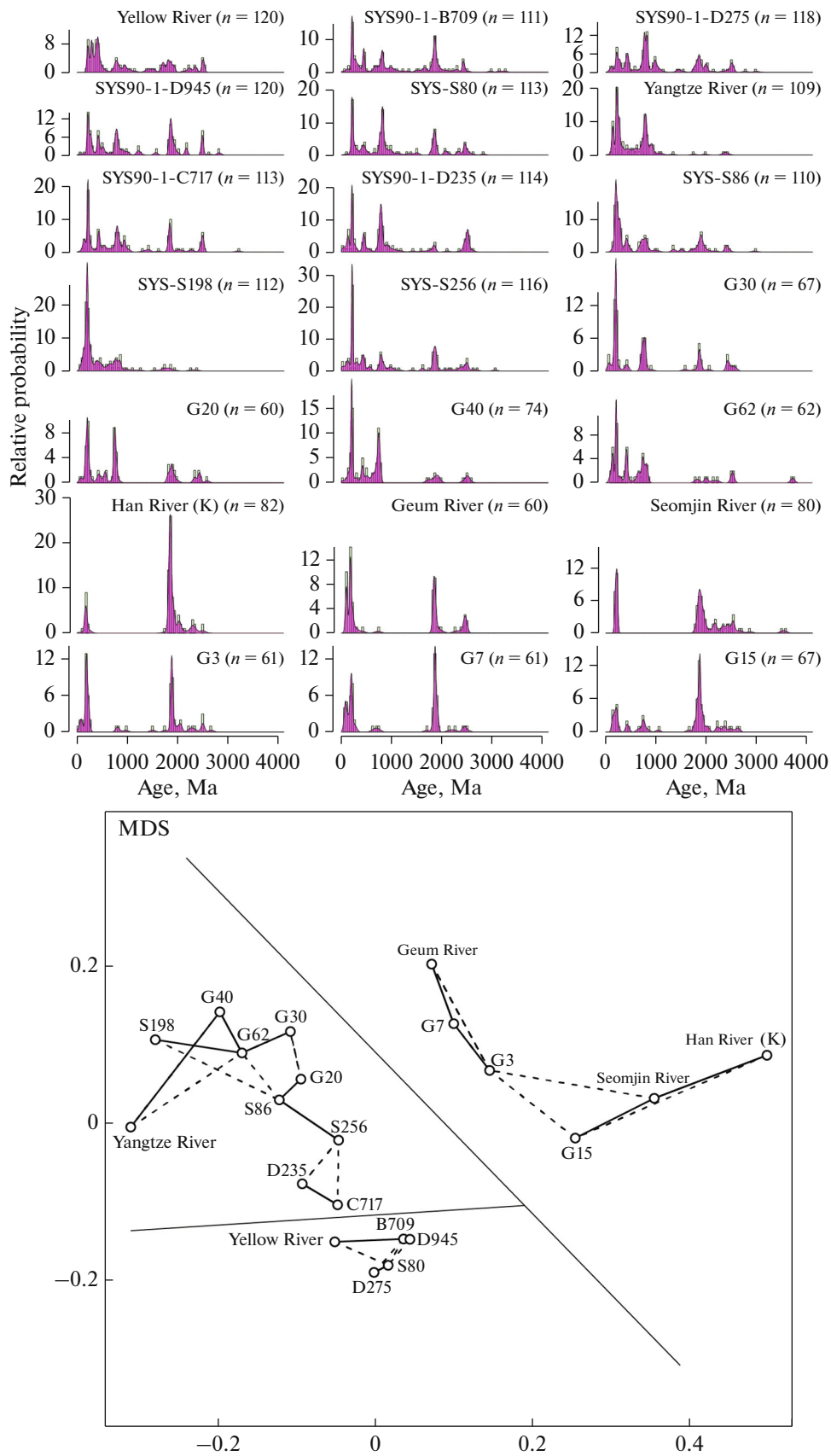


Fig. 3. KDE chart and MDS chart of all studied samples and surrounding river samples.

about 1.0 Ma, indicating that transgression has occurred in where SYS90-1 borehole located since 1 Ma. The U-Pb age spectrum of detrital zircon from the depth 56.20 to 68.88 m in the second part is similar to that of the Yangtze River sediments, indicating that the Yangtze River sediments contributed a lot to the study area during this period. The age of the sediments from 56.20 to 68.88 m was determined to be 0.59–0.71 Ma by astronomical dating tuning. Comparing the curve of global sea level change (Fig. 4), the sediment of SYS90-1 borehole was mainly controlled by the Yangtze River as the sea level decreased and the Yangtze River advanced seaward during this period. In addition, this period was the Gongzi-Minde interglacial age, which further increased the sediment flux into the sea. In the third part, from the depth 56.20 m to the top of the borehole, the sediments mainly came from the Yellow River. Due to the rising sea level, the Yellow Sea and Bohai Sea are connected, and the Yellow River sediments are widely diffused in the South Yellow Sea.

4.2.2. Provenance tracing of boreholes sediments since MIS5 stage. Since MIS5, the sedimentary environment of the South Yellow Sea has been basically consistent with the present sedimentary environment, and the sediment provenance is mainly controlled by river evolution, circulation, climate and sea level fluctuation [60].

Lan et al. analyzed rare earth elements and sediments provenance of borehole NT1 in the central muddy area of the South Yellow Sea since the MIS4 stage [34], and found that the Yangtze River played a major role in the deposition of the central muddy area of the South Yellow Sea from the early Late Pleistocene (MIS4) to modern times. The Yellow River, on the other hand, significantly influenced the sedimentation of the South Yellow Sea shelf during the Early Tamaki glaciation (MIS3 and MIS2) in the late Late Pleistocene (Fig. 5). According to the sediment provenance study of NT2 borehole in the southern side of central muddy area [35], the sediments of the South Yellow Sea shelf were mainly transported by the Yangtze River from the early Late Pleistocene to the modern era, and the sediments were mainly transported by the Yellow River during several low sea level periods in the middle and late Middle Pleistocene (MIS6) and MIS4–MIS3.

Yao et al. selected 13 samples from YZ08 borehole in the coastal zone of Jiangsu Province for U-Pb age spectrum analysis, and found that the provenance of the YZ08 borehole sediments was mainly affected by the Yangtze River during MIS5. During the MIS1 and MIS2, it was under the joint influence of the Yangtze River and the Yellow River, and dominated by the Yangtze River. When the Yellow River captured the Huaihe River into the South Yellow Sea, the percentage of Yellow River sediments had increased and surpassed the Yangtze River [37]. Based on the clastic

mineral assemblage characteristics of the SYS-0701 Yangtze sediments and the clay minerals of the SYS-0804 core sediments of the western shelf of the South Yellow Sea, Zhang concluded that the sediments in the western of the South Yellow Sea were mainly from the Yellow River since the MIS5 [42].

From the results of five boreholes distributed from the coastal zone to the central muddy area, it can be found that, with 34.5° N as the boundary, the sediments in the west of the north side of the boundary had been mainly supplied by the Yellow River (Ancient Yellow River) since the late Pleistocene. And in the east of the north side and in most areas of the south side of the boundary, the Yellow River had a great influence on the seabed sediments during the low sea level period (MIS6, MIS4, MIS2), but the Yangtze River had a great influence during the high sea level period (MIS5, MIS3). In the coastal zone of south side, the sediments mainly came from the Yangtze River.

4.2.3. Tracer of Holocene and surface sediment provenance. Previous studies suggested that the Holocene sediments in the central of the South Yellow Sea were mainly supplied by the Yangtze River and the Yellow River. Zhang analyzed the geochemical elements of YNH109 hole in the central muddy area of the South Yellow Sea and found that the Holocene sediments were mainly from the Yangtze River [62]. Based on the changes of environmental magnetic parameters and the correlation between magnetic susceptibility and median grain size of the YSC-10 borehole with a bottom age of 9.0 ka [36], speculated that the sediments from the borehole before 4.8 ka were mainly from the Yellow River, but the influence of Yangtze River was relatively enhanced after then. It is suggested that the magnetic properties of the YSC-10 borehole sediments are dominated by the Yangtze River sediments related to the Yellow Sea warm current since the Middle Holocene.

According to the KDE and MDS charts of all samples in this study, the zircon U-Pb age spectrum of surface sediments SYB80 and the borehole sediments SYS90-1-B709, SYS90-1-D275 and SYS90-1-D945 are similar to that of the Yellow River sediments. The zircon U-Pb age spectrum of the surface sediments SYB86, SYB198, SYB256, G20, G30, G40, G62 and the borehole sediments SYS90-1-C717, SYS90-1-D235 are similar to that of the Yangtze River sediments. The U-Pb zircon age spectrum of the surface sediments G3, G7, and G15 are similar to those of fluvial sediments from the Korean Peninsula. So, it can be inferred that the southern part of the South Yellow Sea roughly bounded by Jeju Island, the sediments in the west side are mainly from China, and the sediments in the east side are mainly from the Korean Peninsula. This boundary roughly coincides with the boundary between the silty area and the sandy area on the eastern South Yellow Sea.

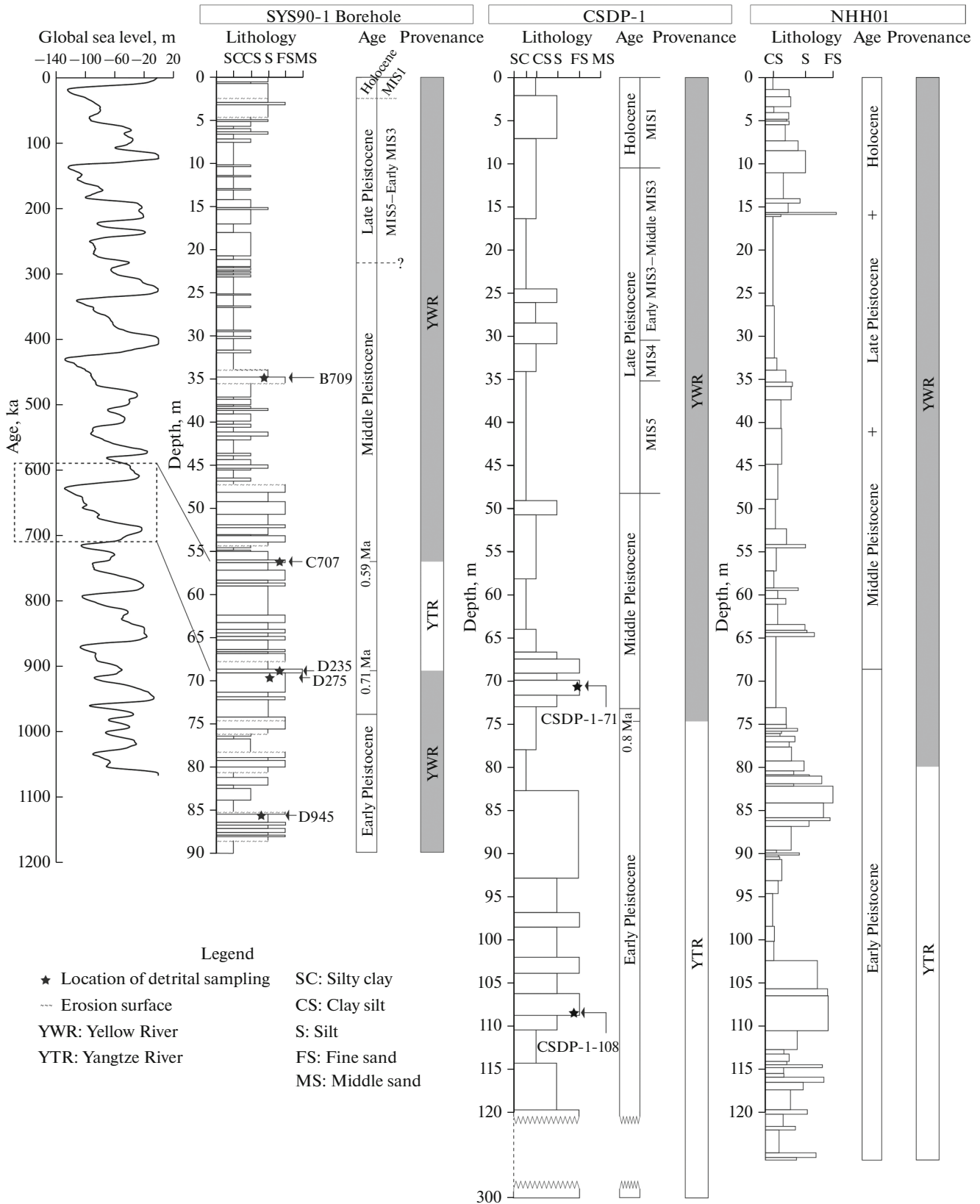


Fig. 4. The change of provenance of typical boreholes.

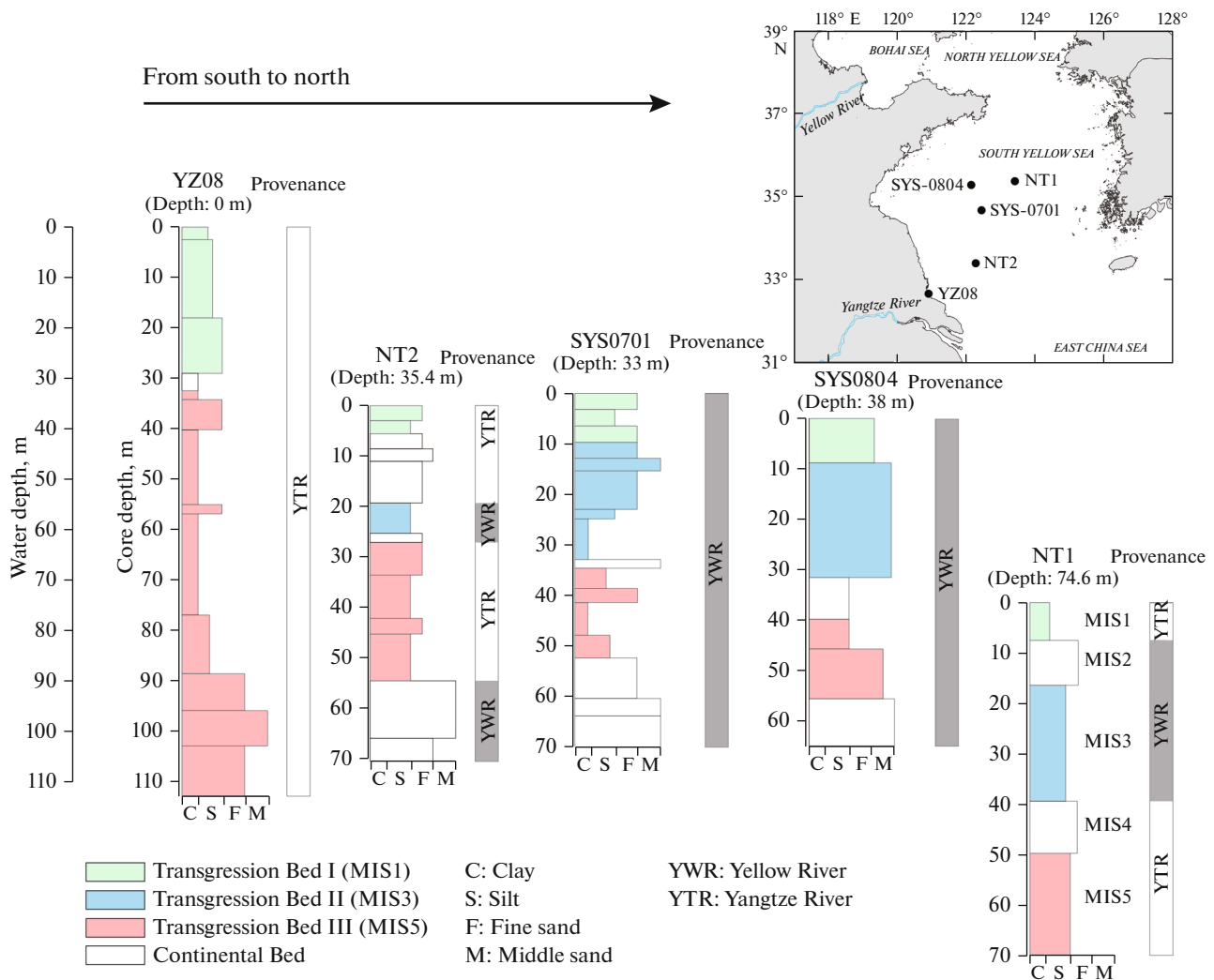


Fig. 5. Schematic diagram of provenance changes in typical Late Pleistocene boreholes (According to reference [61]).

Detrital zircon U-Pb age analysis of surface sediments in the central muddy area shows that it is a mixed sedimentary area, with the Yellow River sediments inner and while the Yangtze River predominates in the southern muddy area. The main control boundary between the Yellow River and the Yangtze River in this region is approximately 33.4° N.

4.3. Response of Provenance Change to Sea Level Change

Since the Holocene, the sediment provenance in the central muddy area of South Yellow Sea has been influenced by many factors, such as sea level change, ocean circulation, East Asian monsoon, river diversion and estuarine delta formation [63–69]. Among them, the circulation system dominated by the Yellow Sea warm current and the coastal current on both sides controls the transport and deposition of input sediments from surrounding rivers [70]. The Yellow Sea

warm current moving northward interacts with the coastal current moving southward to form a cyclonic vortex called cold water mass or cold vortex, which has an obvious control over the formation of the central muddy area of the South Yellow Sea [71]. Many scholars have studied the age of Yellow Sea warm current [9, 64, 72, 73], and limited the time of its entering the South Yellow Sea to 6.9–4.3 ka. The study on environmental magnetic parameters of the cylindrical sediments shows that before the Yellow Sea warm current entered the South Yellow Sea, the sediments may be mainly supplied by the Yellow River, and after then the influence of the Yangtze River sediments increases relatively [36]. The summer monsoon and the Yellow Sea warm current are the main driving forces of Yangtze River sediments. Both of them act on the diluted water of the Yangtze River and transport the sediments to the northwest. The branch rivers of Yangtze River directly transported material to the central mud area during the period of low sea level [19].

The study results of borehole CSDP-1 showed that large-scale transgression occurred in the South Yellow Sea from 0.8 Ma, and the marine environment was close to the present. Before that, the sediments were mainly imported from the Yangtze River [19]. The study results of NHH01 hole [17] show that the signal of Yellow River sediments began to appear after 0.88 Ma, which is consistent with this paper, indicating that the Yellow River sediments began to affect the South Yellow Sea roughly between 0.88 and 1.0 Ma.

Based on the results of the depositional environment comparison and provenance analysis of borehole CSDP-1, NHH01 and SYS90-1A (see Fig. 1 for borehole locations), it can be seen that, in the South Yellow Sea, due to the subsidence of Zhe-Min Uplift during about 1.0–0.83 Ma, seawater entered the South Yellow Sea in the form of “channel” along the Yellow Sea trough from southeast. The phenomenon of “different phenomena at the same time” exists in different regions. During the process of seawater entering the South Yellow Sea, it advances from east to west, reach-

ing SYS90-1 borehole location first, followed by boreholes NHH01 and CSDP-1 location. Limited by insufficient sampling interval, the first appearance of Yellow River sediments in SYS90-1 borehole may be earlier than the current study results.

The Bohai Sea and the Yellow Sea are the main gathering areas of Yellow River sediments. The provenance tracer analysis of borehole sediments from the Bohai Sea and the Yellow Sea has important implications for the study of sea level change in the two sea areas. In this study, it is found that the bottom sediments (about 1.0 Ma) of SYS90-1 borehole was supplied by the Yellow River, indicating that the Yellow River had already flowed eastward into the sea during ~1.0 Ma, and the transgression scale of Yellow Sea and Bohai Sea was probably large at that time. Presently, many scholars have concluded that the Yellow River entered the sea in the early Pleistocene or earlier [74–78]. Xiao et al. studied the detrital zircon age spectra of sediments from three boreholes that penetrated the late Miocene and found that there were significant

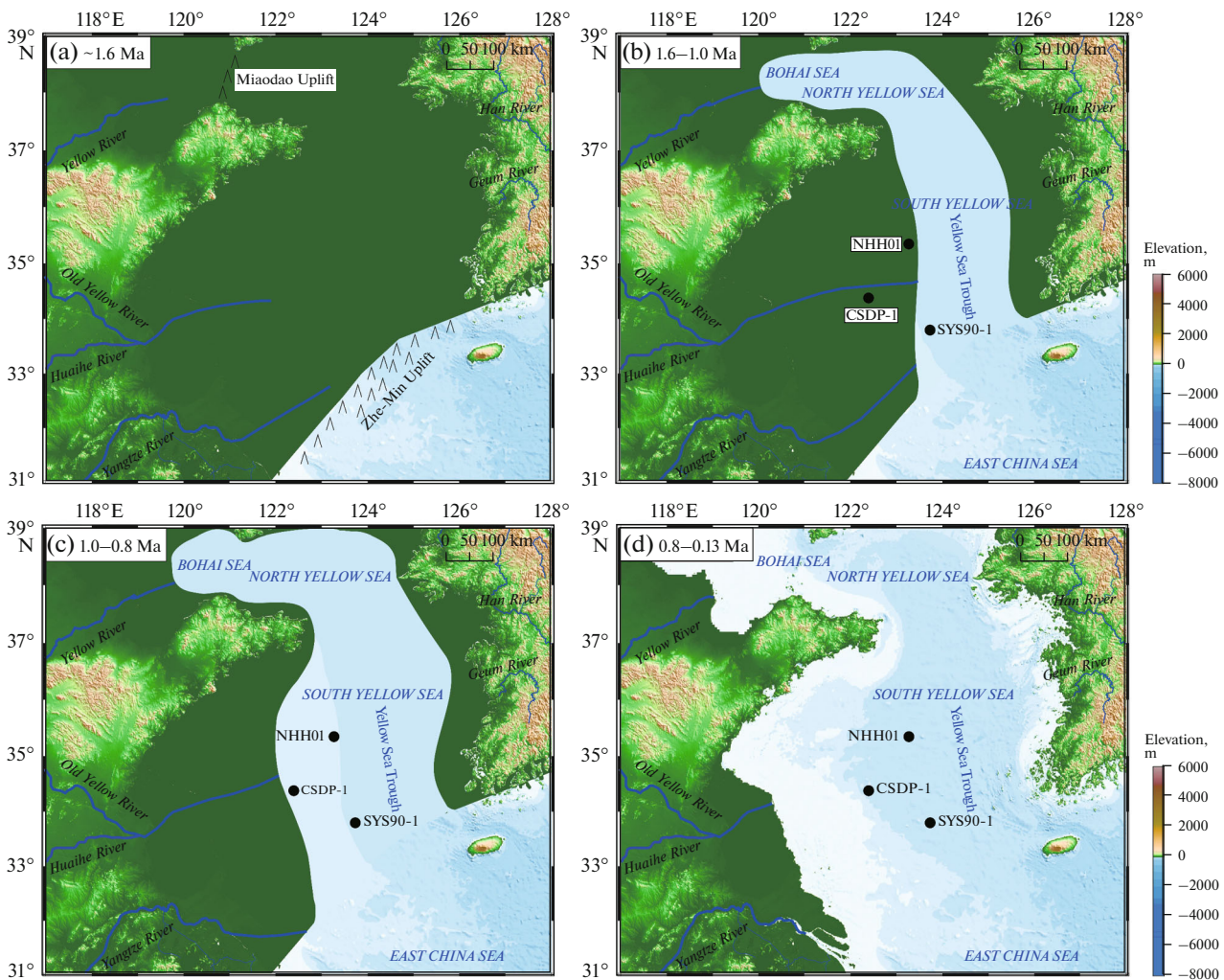


Fig. 6. Transgression process Map of the South Yellow Sea.

provenance changes between 1.6 and 1.5 Ma [79], indicating that the upper and lower reaches of the Yellow River were connected, which provided the possibility for the Yellow River sediments to occur about 1.0 Ma in SYS90-1 borehole. Accordingly, the transgression process of the South Yellow Sea can be inferred (Fig. 6). Before 1.6 Ma, the transgression did not occur in the South Yellow Sea due to the blockage of the Zhe-Min Uplift (Fig. 6a). Subsequently, the Zhe-Min Uplift gradually subsided, and transgression occurred near the Yellow Sea trough at about 1.0 Ma (Fig. 6b) and advanced northward. Then, it gradually advanced westward, reaching the location of NHH01 and CSDP-1 holes at about 0.88 Ma (Fig. 6c). The scope of transgression was basically consistent with the present since late Pleistocene (Fig. 6d).

5. CONCLUSIONS

Before 1.6 Ma, the transgression did not occur in the South Yellow Sea due to the blockage of the Zhe-Min Uplift. During the period from 1.0 to 0.88 Ma, the Zhe-Min Uplift gradually subsided and the seawater entered the South Yellow Sea along the Yellow Sea trough from the southeast to north as a channel, and there were different phenomena at the same time in different regions. Since 0.88 Ma, the sea water has been advancing from east to west. The scope of transgression was basically consistent with the present since late Pleistocene.

The sediments in the western side of Jeju Island are mainly from China, and the sediments in the eastern are mainly from the Korean Peninsula, which roughly coincides with the boundary between the silty area and the sandy area on the east of the South Yellow Sea. In the surface sediments, the boundary between the sediments from Yellow River and the Yangtze River is approximately 33.4° N.

ACKNOWLEDGMENTS

The authors thank the International Cooperation Division of the Ministry of Natural Resources for their support. We gratefully thank Prof. Ziguao Hao and Dr. Xijie Chen from the Development Center of China Geological Survey for their guidance and help. We also thank to Dr. Fanghui Hou and Dr. Yong Yuan of Qingdao Institute of Marine Geology for their guidance on the tectonic evolution of the South Yellow Sea.

FUNDING

This study was funded by the Science and Technology Innovation Project of Laoshan Laboratory (LSKJ202204400), the China Geological Survey Projects (DD20230403, DD20221710, DD2023069) and National Natural Science Foundation of China (41876059).

CONFLICT OF INTEREST

The authors of this work declare that they have no conflicts of interest.

OPEN ACCESS

This article is licensed under a Creative Commons Attribution 4.0 International License, which permits use, sharing, adaptation, distribution and reproduction in any medium or format, as long as you give appropriate credit to the original author(s) and the source, provide a link to the Creative Commons license, and indicate if changes were made. The images or other third party material in this article are included in the article's Creative Commons license, unless indicated otherwise in a credit line to the material. If material is not included in the article's Creative Commons license and your intended use is not permitted by statutory regulation or exceeds the permitted use, you will need to obtain permission directly from the copyright holder. To view a copy of this license, visit <http://creativecommons.org/licenses/by/4.0/>

REFERENCES

1. X. Shi, S. Qiao, S. Yang, J. Li, S. Wan, J. Zou, Z. Xiong, L. Hu, Z. Yao, L. Dong, K. Wang, S. Liu, and Y. Liu, "Progress in sedimentology research of the Asian continental margin (2011–2020)," *Bull. Mineral. Petrol. Geochem.* **40** (2), 319–336 (2021).
2. P. Wang and Z. Jian, "Exploring the deep South China Sea: retrospects and prospects," *Sci. China Earth Sci.* **21** (6), 1473–1488 (2019).
3. S. Yang, "Advances in sedimentary geochemistry and tracing applications of Asian rivers," *Adv. Earth Sci.* **21** (6), 648–655 (2006).
4. X. Qin, X. Shi, Y. Zhang, X. Li, J. Li, G. Xiao, Z. Xu, H. Wang, W. Lv, H. Wu, Y. Yao, L. Shang, C. Yang, Z. Wang, H. Gao, M. Wang, B. Mi, H. Zhong, G. Hu, H. Chen, L. Huang, W. Luo, X. Mei, Z. Xu, Z. Tian, and Z. Wang, "Main achievements and understanding of 1 : 1 million regional geological survey of China Seas," *Geol. China* **47**(5), 1355–1369 (2020).
5. N. J. Shackleton, M. A. Hall and D. Pate, "Pliocene stable isotope stratigraphy of site 846," *Proc. Ocean Drill. Program, Sci. Res.* **138**, 337–355 (1995).
6. A. C. Mix, J. Le, and N. J. Shackleton, "Benthic foraminiferal stable isotope stratigraphy of Site 846: 0–1.8 Ma," *Proc. Ocean Drill. Progr. Sci. Res.* **138**, 839–856 (1995).
7. Y. Zhang, Y. Yao, X. Li, L. Shang, C. Yang, Z. Wang, M. Wang, H. Gao, X. Peng, L. Huang, X. Kong, J. Wang, B. Mi, H. Zhong, H. Chen, H. Wu, W. Luo, X. Mei, G. Hu, J. Zhang, Z. Xu, Z. Tian, Z. Wang, X. Li, and Z. Wang, "Tectonic evolution and resource-environmental effect of China Seas and adjacent areas under the multisphere geodynamic system of the East Asia ocean-continent convergent belt since Mesozoic," *Geol. China*, **47** (5), 1271–1309 (2020).
8. S. Yang, H. Jung, D. Lim, and C. Li, "A review on the provenance discrimination of sediments in the Yellow Sea," *Earth-Sci. Rev.* **63** (1–2), 93–120 (2003).

9. A. C. Liu, S. Li, S. Wang, Z. Yang, Z. Ge, and H. Jeong, "Sea level changes of the Yellow Sea and formation of the Yellow Sea warm current since the last deglaciation," *Mar. Geol. & Quatern. Geol.* **19** (1), 13–24 (1999).
10. J. Liu, Z. Duan, X. Mei, Q. Liu, X. Zhang, X. Guo, Z. Wu, H. Wang, F. Wang, B. Chen, X. Zhang, and Y. An, "Stratigraphic classification and sedimentary evolution of the late Neogene to Quaternary sequence on the Central Uplift of the South Yellow Sea," *Mar. Geol. Quatern. Geol.* **41** (5), 48–58 (2021).
11. J. Lu and A. Li, "Seasonal variations and influencing factors of the grain size characteristics of surface sediments in the South Yellow Sea," *Mar. Sci.* **39** (3), 48–58 (2015).
12. Y. Qin, Y. Zhao, and L. Chen, *Geology of the Yellow Sea* (Oceanic Publish House, Beijing, 1989) [in Chinese].
13. J. Wei, X. Shi, C. Xin, and H. Zhang, "Clay mineral distributions in the southern Yellow Sea and their significance," *Chin. Sci. Bull.* **48** (1), 7–11 (2003).
14. X. Mei, X. Li, B. Mi, L. Zhao, Z. Wang, H. Zhong, H. Yang, X. Huang, M. He, W. Xiong, and Y. Zhang, "Distribution regularity and sedimentary differentiation patterns of China seas surface sediments," *Geol. China* **47** (5), 1447–1462 (2020).
15. J. D. Milliman and K. L. Farnsworth, *River Discharge to the Coastal Ocean: A Global Synthesis* (Cambridge University Press, Cambridge, 2011).
16. S. Qiao, X. Shi, G. Wang, L. Zhou, B. Hu, L. Hu, G. Yang, Y. Liu, Z. Yao, and S. Liu, "Sediment accumulation and budget in the Bohai Sea, Yellow Sea and East China Sea," *Mar. Geol.* **390**, 270–281 (2017).
17. Z. Yao, X. Shi, S. Qiao, Q. Liu, S. Kandasamy, J. Liu, Y. Liu, J. Liu, X. Fang, J. Gao, and Y. Dou, "Persistent effects of the Yellow River on the Chinese marginal seas began at least ~880 ka ago," *Sci. Repts.* **7** (1), 1–11 (2017).
18. M. He, X. Mei, X. Zhang, J. Liu, X. Guo, and H. Zheng, "Provenance discrimination of detrital zircon U-Pb dating in the core CSDP-1 in the continental shelf of South Yellow Sea," *J. Jilin Univ.: Earth Sci. Ed.* **49** (1), 85–95 (2019).
19. J. Zhang, S. Wan, P. Clift, J. Huang, Z. Yu, K. Zhang, X. Mei, J. Liu, Z. Han, Q. Nan, D. Zhao, A. Li, L. Chen, H. Zheng, S. Yang, T. Li, and X. Zhang, "History of Yellow River and Yangtze River delivering sediment to the Yellow Sea since 3.5 Ma: tectonic or climate forcing?" *Quatern. Sci. Rev.* **216**, 74–88 (2019).
20. L. Shang, Y. Zhang, Y. Yao, H. Wu, G. Hu, and Z. Tian, "Late Cenozoic evolution of East China continental margin and restoration of plate interaction processes," *Geol. China* **47** (5), 1323–1336 (2020).
21. B. Lei, J. Chen, Z. Wu, Y. Zhang, J. Liang and G. Li, "Density and velocity analysis and seismic reflection model construction of Marine Mesozoic in North Jiangsu and South Yellow Sea Basin," *Oil Geophysical Prospecting* **53**(3), 558–567 (2018).
22. Y. Pang, X. Zhang, G. Xiao, Z. Wen, X. Guo, F. Hou, and X. Zhu, "Structural and geological characteristics of the South Yellow Sea Basin in lower Yangtze block," *Geol. Rev.* **62** (3), 604–616 (2016).
23. F. Hou, X. Guo, Z. Wu, X. Zhu, X. Zhang, J. Qi, B. Wang, Z. Wen, L. Cai, and Y. Pang, "Research progress and discussion on formation and tectonics of South Yellow Sea," *J. Jilin Univ.: Earth Sci. Ed.* **49** (1), 96–105 (2019).
24. M. Ren and Y. Shi, "Sediment discharge of the Yellow River and its effect on sedimentation of the Bohai and Yellow sea," *Sci. Geograph. Sinica* **1** (6), 1–12 (1986).
25. X. Jin and P. Yu, *Tectonics of the Yellow Sea and the East China Sea C.A.O.S.IOCAS (Institute of Oceanology), The Geology of the Yellow Sea and the East China Sea* (Science Press, Beijing, 1982) [in Chinese].
26. Y. Yao, B. Xia, Z. Feng, L. Wang, and X. Xu, "Tectonic evolution of the South Yellow Sea since the Paleozoic," *Petrol. Geol. Exp.* **27** (2), 124–128 (2005).
27. S. Shen, F. Zheng, and W. Liu, "Mesozoic–Cenozoic tectonic features of southeast China continental margin and the tectonic stress field," *Bull. Inst. Geomechan. CAGS*, No. 8, 9–34 (1986).
28. J. Liu, X. Zhang, X. Mei, Q. Zhao, X. Guo, W. Zhao, J. Liu, Y. Saito, Z. Wu, and J. Li, "The sedimentary succession of the last ~3.50 Myr in the western South Yellow Sea: paleoenvironmental and tectonic implication," *Mar. Geol.* **399**, 47–65 (2018).
29. J. Yuan, J. Chen, J. Liang, Y. Zhang, L. Xue, S. Wu, T. Lan, and P. Wu, "Characteristics and hydrocarbon prospects of the Permian sandstone reservoirs of the Laoshan Uplift, South Yellow Sea," *Mar. Geol. Quatern. Geol.* **41** (5), 181–193 (2021).
30. F. Hou, X. Zhu, X. Zhang, Z. Wu, X. Guo, J. Qi, Z. Wen, B. Wang, and X. Meng, "Basic geological characteristics of the East China Sea region and geological–geophysical characterization of some important tectonic boundaries in the region," *Earth Sci. Front.* **29** (2), 281–293 (2022).
31. J. Yan, J. Hu, D. Wang, W. Gong, and X. Liang, "The critical geological events in the Huang–Huai–Hai Plain during the Late Cenozoic," *Geol. Bull. China* **40** (5), 623–648 (2021).
32. D. Xu, X. Liu, X. Zhang, T. Li, and B. Chen, *China Offshore Geology* (Geological Publishing House, Beijing, 1997) [in Chinese].
33. Z. Liu, B. Liu, Z. Huang, B. Zhu, M. Fu, J. Yan, X. Zhang, and Y. Zheng, *Topography and Geomorphology of China's Offshore and Adjacent Areas* (Oceanic Publish House, Beijing, 2005) [in Chinese].
34. X. Lan, X. Zhang, G. Zhao, and Z. Zhang, "Distributions of rare earth elements in sediments from Core NT1 of the South Yellow Sea and their provenance discrimination," *Geochimica* **38** (2), 123–132 (2009).
35. X. Lan, Z. Zhang, R. Li, and D. Ding, "Provenance study of sediments in core NT2 of the South Yellow Sea," *Acta Sedimentol. Sinica* **28** (6), 1182–1189 (2010).
36. G. Liu, X. Han, Y. Chen, B. Hu, and L. Yi, "Magnetic characteristics of core YSC-10 sediments in the central Yellow Sea mud area and implications for provenance changes," *Acta Sedimentol. Sinica* **39** (2), 383–394 (2021).
37. R. Yao, K. Jiang, Y. Yao, and P. Wang, "Analysis of sediment source of the South Huanghai Sea Shelf since the

- Late Pleistocene,” *Mar. Sci. Bull.* **41** (2), 189–199 (2022).
38. T. Choi, Y. I. Lee, Y. Orihashi, and H. Yi, “The provenance of the southeastern Yellow Sea sediments constrained by detrital zircon U-Pb age,” *Mar. Geol.* **337**, 182–194 (2013).
 39. B. Mi, Y. Zhang, X. Mei, X. Qiu, W. Zhao and X. Lan, “The rare earth element content in surface sediments of coastal areas in eastern China’s sea areas and an analysis of material sources,” *Geol. China* **47** (5), 1530–1541 (2020).
 40. J. Su, “A review of circulation dynamics of the coastal oceans near China,” *Acta Oceanol. Sinica* **23** (3), 1–16 (2001).
 41. X. Mei, X. Zhang, J. Liu, Z. Wang, X. Guo, and X. Huang, “Elemental geochemical record of land and sea environmental evolution since 3.50 Ma in South Yellow Sea,” *J. Jilin Univ.: Earth Sci. Ed.* **49** (1), 74–84 (2019).
 42. J. Zhang, J. Liu, X. Kong, G. Xu, J. Qiu, B. Yue, and F. Wang, “Stratigraphic sequence and depositional environment since marine isotope stage 6 in the continental shelf of the western South Yellow Sea: a case of SYS-0804 core,” *Mar. Geol. Quatern. Geol.* **35** (1), 1–12 (2015).
 43. T. Stevens, A. Carter, T. P. Watson, P. Vermeesch, S. Ando, A. F. Bir, H. Lu, E. Garzanti, M. A. Cottam and I. Sevastjanov, “Genetic linkage between the Yellow River, the Mu Us desert and the Chinese Loess Plateau,” *Quatern. Sci. Rev.* **78**, 355–368 (2013).
 44. P. Vermeesch and E. Garzanti, “Making geological sense of “Big Data” in sedimentary provenance analysis,” *Chem. Geol.* **409**, 20–27 (2015).
 45. X. Tang, S. Guo, X. Xiong, M. Ji, L. Wang, and J. Guo, “Zircon U-Pb dating of the basement granite in the Qiongdongnan Basin, northern South China Sea,” *Geol. China* **49** (1), 336–338 (2022).
 46. V. A. Zaika and A. A. Sorokin, “Age and sources of Dzhagdy Terrane metasedimentary rocks in the Mongol–Okhotsk Fold Belt: detrital zircon U-Pb and Lu-Hf isotopic data,” *Russ. J. Pac. Geol.* **14**, 20–31 (2020). <https://doi.org/10.1134/S181971402001008X>
 47. Y. N. Smirnova, R. O. Ovchinnikov, Y. V. Smirnov, and S. I. Dril, “Sources of sediment clasts and depositional environment of sedimentary rocks of the Daur Series of the Argun continental massif,” *Russ. J. Pac. Geol.* **16**, 11–28 (2022). <https://doi.org/10.1134/S1819714022010092>
 48. C. M. Fedo, K. N. Sircombe, and R. H. Rainbird, “Detrital zircon analysis of the sedimentary record,” *Rev. Mineral. Geochem.* **53** (1), 277–303 (2003).
 49. G. E. Gehrels, V. A. Valencia, and J. Ruiz, “Enhanced precision, accuracy, efficiency, and spatial resolution of U-Pb ages by laser ablation-multicollector-inductively coupled plasma-mass spectrometry,” *Geochim., Geophys., Geosyst.* **9** (3), Q03017 (2008). <https://doi.org/10.1029/2007GC001805>
 50. B. Shaulis, T. J. Lapen, and A. Toms, “Signal linearity of an extended range pulse counting detector: applications to accurate and precise U-Pb dating of zircon by laser ablation quadrupole ICP-MS,” *Geochim., Geophys., Geosyst.* **11** (11), Q0AA11 (2010). <https://doi.org/10.1029/2010GC003198>
 51. W. Compston, I. S. Williams, J. L. Kirschvink, Z. Zhang and M. A. Guogan, “Zircon U-Pb ages for the Early Cambrian time-scale,” *J. Geol. Soc.* **149** (2), 171–184 (1992).
 52. J. Ren, “The new generation geotectonic map of China-geotectonic map of China and adjacent areas (1 : 5000000) a brief description: Chinese geotectonics in a global view,” *Acta Geosci. Sin.* **24** (1), 1–2 (2003).
 53. L. Shao, C. Li, S. Yang, C. Kang, J. Wang, and T. Li, “Neodymium isotopic variations of the late Cenozoic sediments in the Jiangnan Basin: implications for sediment source and evolution of the Yangtze River,” *J. Asian Earth Sci.* **45**, 57–64 (2012).
 54. M. He, H. Zheng, and J. Jia, “Detrital zircon U-Pb dating and Hf isotope of modern sediments in the Yangtze River: implications for the sediment provenance,” *Quatern. Sci.* **33** (4), 656–670 (2013).
 55. Z. Xu, L. Hou, and Z. Wang, *Orogenic Processes of the Songpan Ganze Orogenic Belt of China* (Geological Publishing House, Beijing, 1992) [in Chinese].
 56. B. Yue and J. Liao, “Provenance study of Yellow River sediments by U-Pb dating of the detrital zircons,” *Mar. Geol. Quatern. Geol.* **36** (5), 109–119 (2016).
 57. X. Lin, J. Liu, Z. Wu, B. Yue, and Y. Dong, “U-Pb age characteristics of major fluvial detrital zircons in the Bohai Bay Basin and their provenance implications,” *Mar. Geol. Quatern. Geol.* **41** (2), 136–145 (2021).
 58. P. Vermeesch, “IsoplotR: a free and open toolbox for geochronology,” *Geosci. Front.* **9** (5), 1479–1493 (2018). <https://doi.org/10.1016/j.gsf.2018.04.001>
 59. P. Vermeesch, “Multi-sample comparison of detrital age distributions,” *Chem. Geol.* **341**, 140–146 (2013).
 60. Z. Chen, J. Zhang, S. Shen, M. Huang, J. Xu, H. Ge, and S. M. Jowitt, “Multi-stratigraphic study and response to sea-level fluctuations since the last deglaciation detected from BZK0402 core in the Shuiyang River basin, Yangtze River,” *Geol. China* **49** (2), 655–666 (2022).
 61. Z. Wang, J. Zhang, X. Mei, X. Chen, L. Zhao, Y. Zhang, Z. Zhang, X. Li, R. Li, K. Lu, R. Sun, and S. Yang, “The stratigraphy and depositional environments of China’s sea shelves since MIS5 (74–128) ka,” *Geol. China* **47** (5), 1370–1394 (2020).
 62. X. Zhang, *Holocene Sedimentary Characteristics and Provenance Analysis of the Central and Western South Yellow Sea* (Ocean University of China, Qingdao, 2008) [in Chinese].
 63. L. Yi, S. Chen, J. D. Ortiz, G. Chen, J. Peng, F. Liu, Y. Chen, and C. Deng, “1500-year cycle dominated Holocene dynamics of the Yellow River delta, China,” *The Holocene* **26** (2), 222–234 (2016).
 64. G. Kong, S. Park, H. Han, J. Chang, and A. Mackensen, “Late Quaternary paleoenvironmental changes in the southeastern Yellow Sea, Korea,” *Quatern. Int.* **144** (1), 38–52 (2006).
 65. X. Zhou, L. Sun, W. Huang, Y. Liu, N. Jia, and W. Cheng, “Relationship between magnetic susceptibility and grain size of sediments in the China Seas and its implications,” *Cont. Shelf Res.* **72**, 131–137 (2014).

66. J. Liu, J. D. Milliman, S. Gao, and P. Cheng, "Holocene development of the Yellow River's subaqueous delta, North Yellow Sea," *Mar. Geol.* **209** (1–4), 45–67 (2004).
67. B. Hu, Z. Yang, M. Zhao, Y. Saito, D. Fan, and L. Wang, "Grain size records reveal variability of the East Asian Winter Monsoon since the Middle Holocene in the Central Yellow Sea mud area, China," *Sci. China Earth Sci.* **55** (10), 1656–1668 (2012).
68. X. Zhou, L. Sun, W. Huang, W. Cheng, and N. Jia, "Precipitation in the Yellow River drainage basin and East Asian monsoon strength on a decadal time scale," *Quatern. Res.* **78** (3), 486–491 (2012).
69. X. Zhou, N. Jia, W. Cheng, Y. Wang, and L. Sun, "Relocation of the Yellow River estuary in 1855 AD recorded in the sediment core from the northern Yellow Sea," *J. Ocean Univ. China* **12** (4), 624–628 (2013).
70. C. E. Naimie, C. A. Blain, and D. R. Lynch, "Seasonal mean circulation in the Yellow Sea: a model-generated climatology," *Cont. Shelf Res.* **21** (6–7), 667–695 (2001).
71. F. Wang, J. Liu, J. Qiu, X. Liu, and X. Mei, "Thickness variation and provenance of Mid-Holocene mud sediments in the central and western South Yellow Sea," *Mar. Geol. Quatern. Geol.* **34** (5), 1–11 (2014).
72. T. Li, S. Li, S. Cang, J. Liu, and H. C. Jeong, "Paleo-hydrological reconstruction of the southern Yellow Sea inferred from foraminiferal fauna in core YSDP102," *Oceanol. Limnol. Sinica* **31** (6), 588–595 (2000).
73. L. Wang, Z. Yang, X. Zhao, L. Xing, M. Zhao, Y. Saito, and D. Fan, "Sedimentary characteristics of core YE-2 from the central mud area in the South Yellow Sea during last 8400 years and its interspace coarse layers," *Mar. Geol. Quatern. Geol.* **29** (5), 1–11 (2009).
74. B. Yuan and Z. Wang, "Uplift of the Qinghai–Xizang Plateau and the Yellow River physiographic period," *Quatern. Sci.*, No. 4, 353–359 (1995).
75. S. Yang, J. Cai, C. Li, and B. Deng, "New discussion about the run-through time of the Yellow River," *Mar. Geol. Quatern. Geol.* **21** (2), 15–19 (2001).
76. Z. Zhu, "The formation of river terraces and evolution of drainage system in the middle Yellow River," *Acta Geogr. Sinica* **44** (4), 429–440 (1989).
77. S. Cheng, Q. Deng, W. Min, and G. Yang, "Yellow River and Quaternary tectonic movements of the Ordos Plateau," *Quatern. Sci.*, No. 3, 238–248 (1998).
78. Y. Lei, L. He, S. Ye, L. Zhao, H. Yuan, S. Yang, C. Xue, and E. A. Laws, "Paleochannel distribution, delta development and paleoenvironment evolution in Bohai Bay since the Late Pleistocene," *Geology in China* **48**(6), 1947–1964 (2021)..
79. G. Xiao, Y. Sun, J. Yang, Q. Yin, G. Dupont-Nivet, A. Licht, A. E. Kehew, Y. Hu, J. Geng, G. Dai, Q. Zhao, and Z. Wu, "Early Pleistocene integration of the Yellow River I: Detrital-zircon evidence from the North Chain Plain," *Palaeogeogr., Palaeoclimatol., Palaeoecol.* **546**, 109691 (2020).

Publisher's Note. Pleiades Publishing remains neutral with regard to jurisdictional claims in published maps and institutional affiliations.